

TOPEX/POSEIDON PRECISE ORBIT DETERMINATION

**A. J. E. Smith, E. T. Hesper, D. C. Kuijper, G. J. Mets,
B. A. C. Ambrosius and K. F. Wakker***

Orbits have been computed for TOPEX/Poseidon from SLR, DORIS, and GPS tracking data. The altimeter data in the form of crossover difference observations have been used for orbit error verification purposes. The RMS of fit of the SLR residuals and an analysis of the orbital overlaps suggest that the TOPEX/Poseidon orbits have a radial accuracy of 3-5 cm. This is confirmed by the radial differences between the various orbit solutions and by the crossover statistics. The latter indicate that, depending on the tracking data used, about 3-4 cm of the orbit error is of a 1-cpr nature. The remainder of approximately 2 cm, which is of gravitational origin, has been found from the calibrated JGM-2 gravity field covariance.

1 Introduction

On August 10, 1992, the TOPEX/Poseidon altimeter satellite was launched from Kourou, French Guiana, into a 10-day repeat orbit with an altitude of 1336 km and an inclination of 66°. The mission which is jointly conducted by the United States' National Aeronautics and Space Administration (NASA) and the French space agency, Centre National d' Etudes Spatiales (CNES), will primarily last for three years with a possible two years extension. The primary goal of the TOPEX/Poseidon mission is to make precise measurements of sea level for the study of global ocean circulation. In order to fully exploit the altimetric data, the satellite's radial ephemeris must be known to subdecimeter accuracy. To meet this stringent orbit requirement, the satellite can potentially make use of five tracking systems: (i) Satellite Laser Ranging (SLR), (ii) one-way Doppler (DORIS), (iii) the Global Positioning System (GPS), (iv) the Tracking and Data Relay Satellite System (TDRSS), and (v) the radar altimeter itself. From this ensemble of tracking systems, only SLR and DORIS are used to compute orbits on a routinely basis. The GPS receiver is still being considered experimental and will have to demonstrate the use of GPS for the orbit determination of low-earth satellites. The carrier signal of the S-band communications link with the TDRSS satellite constellation, which is used to telemeter the scientific and housekeeping data to earth, is not expected to give the highly accurate orbits strived for. The altimetric data, although they have proven their usefulness if tracking data from an SLR network are sparse [1, 2], will be excluded from the orbit computations because of their potential to alias the orbit error into the sea level that TOPEX/Poseidon is trying to measure.

This paper presents some results of TOPEX/Poseidon orbit computations performed at Delft University of Technology, Section Space Research and Technology (DUT/SSR&T) from three of these tracking data types, i.e. SLR, DORIS, and GPS. The altimeter observations have been used for orbit error verification purposes.

* Section Space Research and Technology, Delft University of Technology, Kluyverweg 1, NL-2629 HS Delft, The Netherlands.

2 Orbit computations from SLR and DORIS tracking data

At DUT/SSR&T, the SLR and DORIS data are processed with the GEODYN II software developed by the Wolf Research and Development Group (EG&G) under NASA contract. The arc length over which the orbits are computed was chosen equal to the TOPEX/Poseidon repeat cycle including a one day overlap, i.e. 10.9-day arcs. The data are imported from the Crustal Dynamics Data and Information System (CDDIS) at Goddard Space Flight Center (GSFC). The actual distribution of the DORIS data is performed by CNES.

The accuracy with which the TOPEX/Poseidon orbits have to be computed imposes high demands on the applied orbit computation methodology and the used tracking system. To meet the orbit requirements of TOPEX/Poseidon, the effects of conservative and non-conservative forces on the satellite have to be modeled with extreme accuracy. Therefore, the most up-to-date models are used in the orbit computations. For the gravity field this is the post-launch JGM-2 model complete to degree and order 70 which has been obtained from JGM-1 using 15 cycles of SLR and DORIS data on TOPEX/Poseidon [3]. The Box-Wing Model was applied to account for the satellite's complex geometry, and attitude and surface properties in the modeling of solar radiation pressure and atmospheric drag [3]. For the latter, the French DTM density model with 3-hourly planetary geomagnetic index (Kp) values has been adopted. Also incorporated in the orbit computations are models for solid earth and ocean tides, the earth's albedo radiation pressure, relativity, and n-body perturbations from the sun, the moon, and the planets.

During the orbit computations, drag and solar radiation forces are held constant at nominal values. Model mismatches introduced by this approach are absorbed by a daily estimated set of 1 cycle per revolution (cpr) accelerations in the along-track and cross-track directions, and an additional constant acceleration in the along-track direction. Along with the epoch state vector, pass-dependent range-rate biases and tropospheric scale biases are estimated for the DORIS data. In addition, estimates for inaccurately known coordinates of SLR stations are included in the orbit determination.

An important factor that influences the orbit accuracy and therefore should be mentioned is the geographic and temporal distribution of the tracking data. Currently, the SLR data are provided by a worldwide tracking network of over 30 stations. A number of these stations, 16 in total, form the primary network that was selected as the baseline configuration in support of the mission [3]. The data acquired by the other SLR stations are used in the orbit computations nonetheless. The DORIS data are supplied by a worldwide network of over 45 ground beacons. The fact that the isotropic distribution of the DORIS network and its all-weather capability enable the DORIS system to provide a nearly continuous monitoring of the TOPEX orbit, may serve as evidence that the geographic and temporal distribution of the DORIS tracking data are quite satisfactory. This in contrast with the distribution of the SLR network, which is concentrated on the northern hemisphere, particularly in Europe and North America. Figure 1 and Figure 2 illustrate the geographic distribution of the DORIS network and the SLR network respectively.

For the first 25 cycles of TOPEX/Poseidon, orbits have been computed from SLR data using both the field-generated normal points and the sampled full-rate measurements (a mere 5 % of the data). For this period, a total of 99135 quick-look SLR measurements were available for the orbit computations. On average, 16 passes were collected per day by the SLR systems. Outliers, bad passes, and passes with a significant timing or range bias are eliminated from the orbit computation process during the processing of the SLR data. The weight sigma assigned to each SLR station is a Root Sum Square (RSS) combination of the assumed overall model accuracy (5 cm) and a system dependent noise level. At the moment, the best instruments provide SLR measurements with a precision of better than a centimeter.

For cycle 14 (January 30 to February 8, 1993) and cycles 20 through 25 (March 30 to May 29, 1993), orbits have been computed from DORIS data and a combination of SLR and DORIS data. The resulting solutions for the epoch state vector and general accelerations as obtained from SLR were used as a-priori values in the orbit computations based on DORIS tracking data only, to prevent the

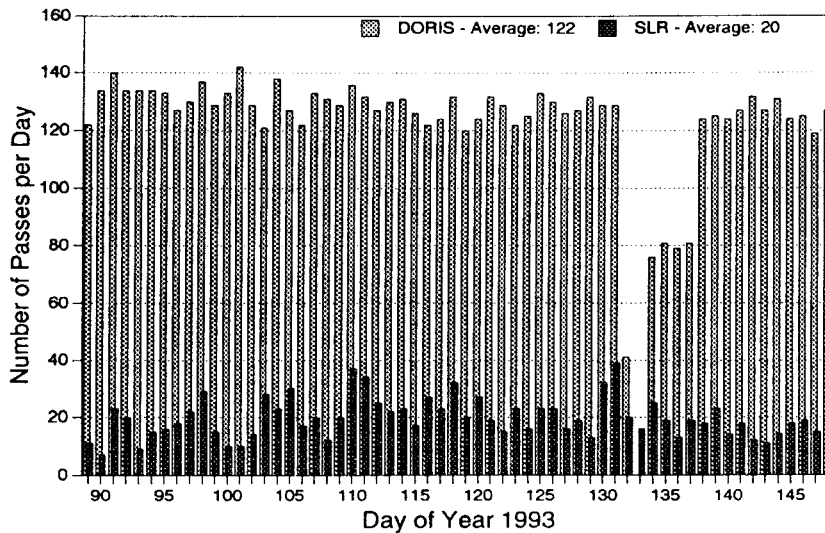


Figure 3. Number of SLR and DORIS passes per day for cycles 20 through 25.

Table 1. RMS of fit of SLR and DORIS tracking data for the SLR, DORIS, and SLR/DORIS orbit solutions of cycle 14 and cycles 20 through 25. (RMS of fit in cm for SLR and in mm/s for DORIS).

Cycle	SLR	DORIS	SLR/DORIS	
			SLR	DORIS
14	4.9	0.57	5.0	0.58
20	4.5	0.57	4.9	0.58
21	5.2	0.56	4.6	0.57
22	4.6	0.54	5.0	0.56
23	4.8	0.57	4.7	0.58
24	5.2	0.52	4.2	0.53
25	4.3	0.55	4.4	0.56
Mean	4.9 ± 0.3	0.55 ± 0.02	4.7 ± 0.3	0.57 ± 0.02

in the TOPEX/Poseidon orbit determination. It is observed that the range-rate residual RMS for the DORIS only orbits is about 0.55 mm/s and does not deviate much from this value. The same applies to the DORIS residual RMS of the SLR/DORIS orbit solutions. The SLR residual RMS for the SLR only and SLR/DORIS orbits have a mean of 4.9 and 4.7 cm respectively, with more or less the same standard deviation of 0.3 cm. When the results for the first 19 cycles of TOPEX/Poseidon SLR orbits are included, a mean residual RMS of 4.6 cm with a standard deviation of 0.5 cm is found.

Another measure for the quality of an orbit is the RMS radial overlap. This quantity which is defined as the RMS of the radial orbit differences between the last day and the first day of adjacent orbital arcs, gives an indication of how much the orbit shifts from one arc to the next to accommodate force and measurement model errors. The results for the orbital overlaps are presented in Table 2. Notice that the DORIS orbits are generally more consistent than the SLR orbits, and that on average, the RMS orbital overlap is better than 3 cm.

Individually, quantities like the RMS radial overlap and the RMS of fit of the residuals are not sufficient to assess the orbit accuracy. Correlated errors are namely eliminated from the orbital

Table 2. RMS radial overlap (cm) of SLR, DORIS, and SLR/DORIS orbit solutions for cycles 20 through 25.

Cycles	SLR	DORIS	SLR/DORIS
20-21	7.0	1.4	3.8
21-22	2.2	1.0	1.2
22-23	3.3	1.4	3.9
23-24	2.0	2.3	2.3
24-25	1.8	2.6	1.9
Mean	3.3 ± 2.2	1.7 ± 0.7	2.6 ± 1.2

overlaps whereas the RMS of fit is based on data residuals that were minimized in the orbit computations. Together however, these quantities provide a good measure for the orbit quality indicating that the TOPEX/Poseidon orbits have a radial accuracy of 3-5 cm.

3 Orbit computations from GPS tracking data

For cycle 14, TOPEX/Poseidon orbits have been computed from the data obtained by the GPS Demonstration Receiver (GPSDR) on TOPEX/Poseidon and by a network of 10 globally distributed ground receivers. Half the number of these receivers have accurately known station coordinates and form the so-called fiducial network for cycle 14. The data from the fiducial network are included to constrain the TOPEX/Poseidon orbit to the terrestrial reference frame. This could not be accomplished by the GPS constellation because the orbits of the GPS satellites are estimated along in the TOPEX/Poseidon orbit determination at DUT/SSR&T. The GPS measurements are processed in ten 30-hour contiguous solution arcs with a 6-hour overlapping period using the GIPSY-OASIS II (GPS Inferred Positioning SYstem - Orbit Analysis and Simulation Software II) software system, developed at the Jet Propulsion Laboratory (JPL) in Pasadena, California. Basically, two estimation strategies have been investigated. The first is a dynamic technique, which relies on the accuracy of the dynamic models and is characterized by the fact that the transition of the satellite state at different observation times is accomplished by the integration of the equations of motion. The second is a so-called reduced-dynamic technique, which takes full advantage of the geometric information content available from the GPS measurements and therefore is less dependent on the precision of the dynamic models. This technique is based on the fact that the satellite state transition at different observation times is accomplished by both the integration of the equations of motion and by the satellite positional change inferred from continuous GPS carrier phase measurements.

The GPSDR onboard TOPEX/Poseidon is the first highly sophisticated space-borne GPS receiver that can actually record both carrier phase and pseudo-range measurements at an extremely high data rate. The carrier phases are recorded every second, while the pseudo-ranges are recorded every 10 seconds. Since the GPSDR can take measurements from up to six GPS satellites simultaneously, it accordingly provides a continuous, global, and dense set of observations. At any instant of time, these observations are also in several directions. This is obviously an advantage of the GPS tracking system compared to both the SLR and DORIS systems which do not have these abilities [4]. Figure 4 displays the TOPEX/Poseidon ground tracking network for cycle 14, showing a global distribution of the 10 ground stations.

For the orbit computations, the first-order ionosphere-free pseudo-ranges and carrier phase observations are formed which are assigned a data noise of respectively 1 m and 1 cm for the 10 ground receivers, and respectively 3 m and 2 cm for TOPEX/Poseidon. The carrier phase observations are decimated to a data rate of 1 observation per 5 minutes, while the pseudo-range observations are compressed to 5-minute normal points by smoothing them against the carrier over the entire 5-minute interval. For both observation types, a cut-off elevation angle is used of

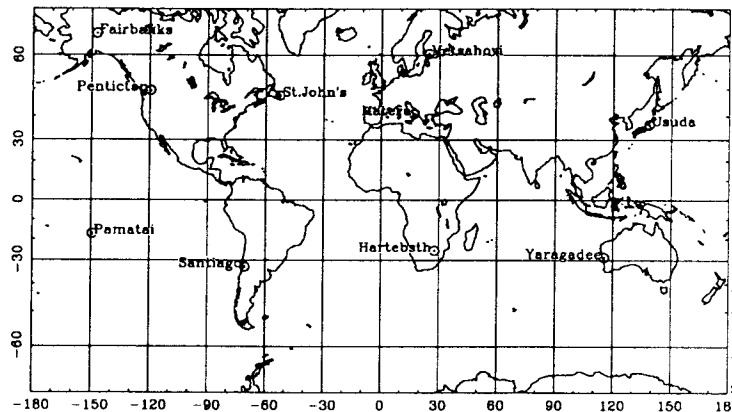


Figure 4. TOPEX/Poseidon GPS ground tracking network for cycle 14.

about 0° for TOPEX/Poseidon and 15° for all ground stations. In the GIPSY-OASIS II software, all measurements are divided into finite discrete time intervals known as batches. The software makes use of a SRIF (Square Root Information Filter) filter, which is a so-called epoch state filter in which all measurements are processed sequentially. The time update of the filter propagates the satellite state estimates and covariances from one batch to the next using a state transition model, while the measurement update of the filter incorporates a new batch of measurements. To obtain the optimal parameter estimates and covariances at all batch observation times from 100% of the measurements, a backward smoothing in time is performed. At the same time, it is possible to perform a forward mapping in time, since the filtered state estimates and covariances apply to the epoch state.

In the TOPEX/Poseidon orbit determination, the JGM-2 gravity field model is used. In comparison, the GEM-T3 model, truncated at degree and order 8, is applied for the computation of the orbits of the GPS satellites. Like the SLR and DORIS orbit determination scheme, the Box-Wing model is adopted for solar pressure, earth radiation, and atmospheric drag on TOPEX/Poseidon. Furthermore, models for solid earth tides, ocean tides, and pole tides are applied. The estimated parameters include the TOPEX/Poseidon state vector at epoch, constant and 1-cpr accelerations in the cross-track and along-track directions for TOPEX/Poseidon, additional 2-cpr cross-track and along-track accelerations, the GPS state vectors at epoch, the constant GPS solar pressure scale factor, the constant and stochastic GPS solar radiation Y-biases, the stochastic GPS solar radiation scaling factors X and Z, the non-fiducial station locations, the random walk modeled tropospheric dry zenith residual delays, the X and Y pole position and corresponding rates, the UT1-UTC rate, the carrier phase biases, the TOPEX/Poseidon receiver clock (modeled as white noise), the GPS transmitter clocks (modeled as white noise) and the ground receiver clocks (modeled as white noise) except for one reference clock. The initial value for the epoch state vector of TOPEX/Poseidon is obtained from the SLR data processing. Furthermore, the GPS orbits of IGS (International GPS Service for Geodynamics) are used as a-priori information for the epoch states of all GPS satellites. These orbits, which have an estimated accuracy of about 30 cm, are a weighted mean of the orbits computed by several different processing centers, viz.

- (i) European Space Operation Centre (ESOC) in Darmstadt, Germany,
- (ii) GeoForschungs Zentrum (GFZ) in Potsdam, Germany,
- (iii) Centre of Orbit Determination Europe (CODE) in Berne, Switzerland,
- (iv) National Geodetic Survey (NGS) in Rockwell, Maryland,
- (v) Jet Propulsion Laboratory (JPL) in Pasadena, California,
- (vi) Scripps Institute of Oceanography (SIO) in La Jolla, California,
- (vii) Energy Mines Resource (EMR) in Ottawa, Canada.

Finally, it is noteworthy to mention that it is possible to specify initial values for the empirical

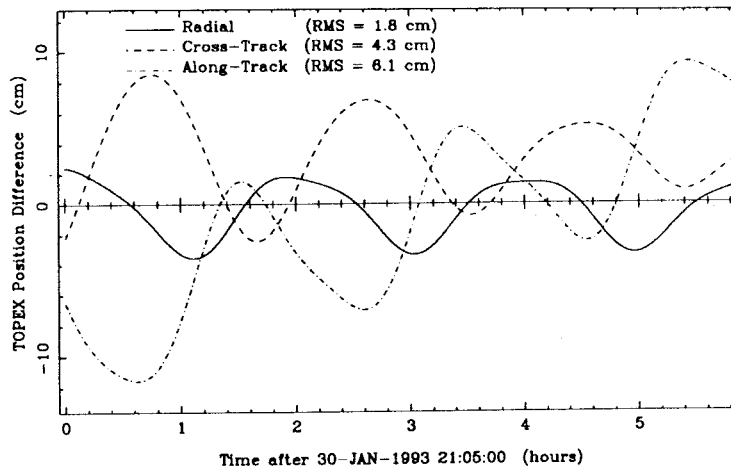


Figure 5. Differences in TOPEX/Poseidon position components over a 6-hour overlap between two 30-hour data arcs using a dynamic technique.

Table 3. RMS of fit summary of the GPS tracking data for cycle 14 using a dynamic technique. (RMS of fit in cm).

Arc Id.	Start Time	Overall		TOPEX/Poseidon	
1	29-JAN-1993 21:00	45.6	0.45	69.9	0.92
2	30-JAN-1993 21:00	43.0	0.48	67.8	0.88
3	31-JAN-1993 21:00	51.1	0.47	68.2	0.90
4	01-FEB-1993 21:00	32.5	0.46	70.3	0.86
5	02-FEB-1993 21:00	29.6	0.40	66.7	0.75
6	03-FEB-1993 21:00	31.4	0.46	70.9	0.88
7	04-FEB-1993 21:00	32.0	0.52	71.2	1.05
8	05-FEB-1993 21:00	34.6	0.53	72.5	1.05
9	06-FEB-1993 21:00	41.3	0.50	68.7	0.96
10	07-FEB-1993 21:00	49.1	0.50	75.2	1.01
Mean		39.0 ± 7.6	0.48 ± 0.04	70.1 ± 2.4	0.93 ± 0.09

accelerations of the custom force model of TOPEX/Poseidon. Information about the constant accelerations and the sine and cosine 1-cpr and 2-cpr terms of the empirical force on TOPEX/Poseidon, can be obtained by first performing a dynamic filtering where these parameters are solved for. Then, the solved-for empirical force terms can be kept fixed in a subsequent reduced-dynamic filtering.

To obtain an indication of the TOPEX/Poseidon orbit accuracy, the observation residuals and the ephemeris differences over the 6-hour orbital overlaps have been investigated. Starting with the results of the dynamic technique, Figure 5 shows the TOPEX/Poseidon ephemeris differences in the radial, cross-track, and along-track directions over a typical 6-hour overlapping period. Since the RMS difference is about 2 cm radial, 4 cm cross-track, and 6 cm along-track, it may be concluded that subdecimeter orbit accuracy can already be achieved with the dynamic filtering. The residual summary for cycle 14 using the dynamic technique is listed in Table 3 for the ten 30-hour data arcs that were processed. Columns 3 and 4 give the overall RMS of fit for the first-order ionosphere-free pseudo-ranges and carrier phase observations respectively. In columns 5 and 6, the TOPEX/Poseidon part of the corresponding data types is listed. On average, the number of observations is about 18000 for each data arc and each data type. Roughly 10 % of the observations

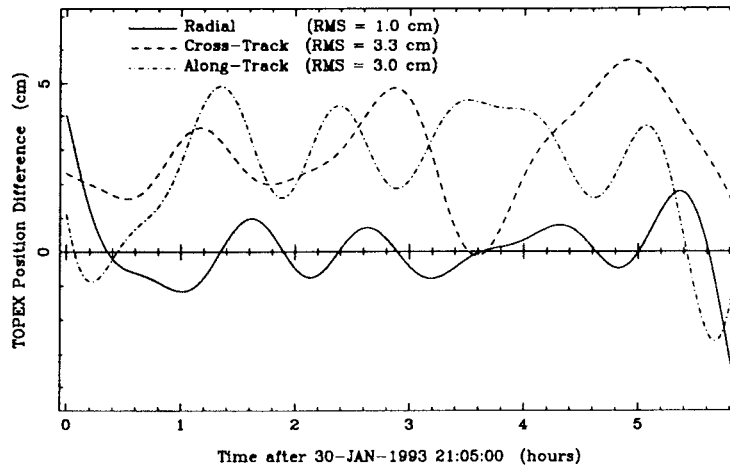


Figure 6. Differences in TOPEX/Poseidon position components over a 6-hour overlap between two 30-hour data arcs using a reduced-dynamic technique.

Table 4. RMS of fit summary of the GPS tracking data for cycle 14 using a reduced-dynamic technique. (RMS of fit in cm).

Arc Id.	Start Time	Overall		TOPEX/Poseidon	
1	29-JAN-1993 21:00	45.6	0.39	68.5	0.46
2	30-JAN-1993 21:00	42.9	0.43	66.9	0.43
3	31-JAN-1993 21:00	51.1	0.41	64.8	0.44
4	01-FEB-1993 21:00	31.8	0.41	66.6	0.43
5	02-FEB-1993 21:00	29.4	0.36	66.0	0.39
6	03-FEB-1993 21:00	30.5	0.41	67.3	0.43
7	04-FEB-1993 21:00	30.7	0.45	65.0	0.47
8	05-FEB-1993 21:00	33.6	0.46	66.5	0.48
9	06-FEB-1993 21:00	40.9	0.45	64.5	0.46
10	07-FEB-1993 21:00	48.2	0.41	67.0	0.46
Mean		38.5 ± 7.8	0.42 ± 0.03	66.3 ± 1.2	0.44 ± 0.03

are taken on TOPEX/Poseidon. As can be seen, the average RMS of fit is approximately 40 cm for the pseudo-ranges and about 0.5 cm for the carrier phases. Considering the TOPEX/Poseidon part of the residual summary, it can be concluded that the RMS of fit of the pseudo-ranges and carrier phases is about 70 cm and 0.9 cm, respectively.

In case of the reduced-dynamic technique, a second filtering was performed to absorb the higher-order dynamic modeling errors. Using this approach, a so-called three-dimensional process-noise force consisting of fictitious accelerations was estimated for TOPEX/Poseidon to absorb the remaining small higher-order dynamic modeling errors. The correlation time of the estimated fictitious accelerations was set to 15 minutes and the corresponding steady-state uncertainty was set equal to the a-priori uncertainty. The uncertainties were assumed to be 10 nm/s^2 in the radial direction and 20 nm/s^2 in both the cross-track and along-track directions, and were taken from [5]. Furthermore, the data noise of the TOPEX/Poseidon carrier phase observations was tightened to 1 cm in order to give the tracking data on TOPEX/Poseidon a higher weight. Figure 6 shows the overlap comparison using reduced-dynamic filtering for the same 6-hour period that is displayed in Figure 5. Obviously, using the reduced-dynamic technique, better results are obtained with an RMS difference in the TOPEX/Poseidon orbit of about 1 cm radial, 3 cm cross-track and 3 cm along-track.

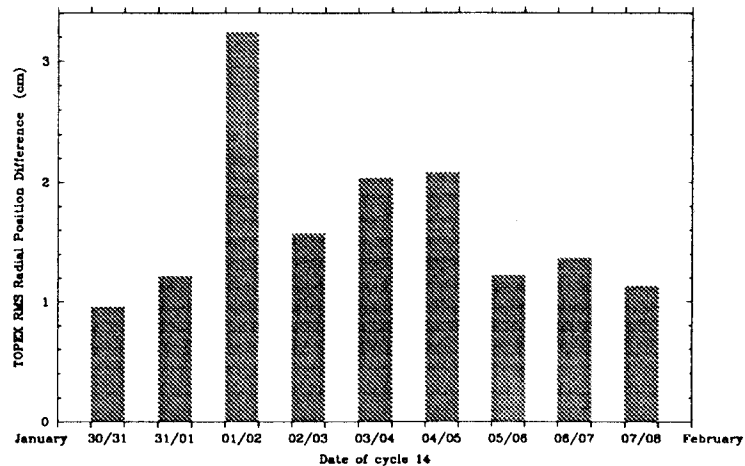


Figure 7. Radial orbit overlap RMS for ten 30-hour consecutive TOPEX/Poseidon data arcs using a reduced-dynamic technique.

The corresponding residual summary for cycle 14 using a reduced-dynamic strategy is shown in Table 4. The overall RMS of fit has only changed significantly for the carrier phase observations to about 0.4 cm. The same observation can be made for the TOPEX/Poseidon part of the summary, showing a decrease of the RMS of fit of the pseudo-ranges to about 66 cm while the RMS of fit of the carrier phase measurements dramatically improved to the 0.4 cm level, which is due to the fact that the remaining higher-order dynamic modeling errors have been absorbed by the three-dimensional process-noise force. Notice that the RMS of fit values of 66 cm and 0.4 cm are close to the noise levels of the first-order ionosphere-free pseudo-range and carrier phase observations on TOPEX/Poseidon, which are about 70 cm and 0.5 cm respectively [6].

Finally, Figure 7 shows the radial RMS overlap results for the 6-hour time periods between consecutive data arcs using a reduced-dynamic filtering. Overall, it is obvious that the RMS radial overlap is about 1.5 cm, which is of the same order of magnitude as the estimated 1-2 cm precision of the altimeter measurements [3].

4 Orbit error assessment

From the previous Sections, the RMS of fit of the SLR residuals and the RMS radial overlap of the various orbit solutions indicate that the TOPEX/Poseidon orbits are accurate to 3-5 cm in the radial direction. This estimate can be verified by the analysis of data that were not included in the orbit computations. For this purpose, the altimeter observations have been used in the form of so-called crossover residuals.

Because a crossover residual is computed by subtracting two interpolated altimeter height residuals at the same geographic location, correlated errors like those resulting from the geoid will be eliminated at the crossovers. In contrast, any error source in the altimeter height observations for which errors on ascending and descending tracks are uncorrelated will propagate into the crossover residual RMS by $\sqrt{2}$. Consequently, assuming that orbit errors on ascending and descending tracks are uncorrelated, a straight forward rule to assess the radial orbit error would be to divide the crossover residual RMS by $\sqrt{2}$. However, for orbits as accurate as in case of TOPEX/Poseidon, the crossover residuals do no longer provide unambiguous information on the orbit error but mainly reflect ocean variability and tidal errors. This is clearly demonstrated by Figure 8 which shows the crossover residual RMS for cycle 14 as a function of the time interval between ascending and descending tracks forming the crossover. Plotted are the GPS reduced-dynamic orbit solution and the

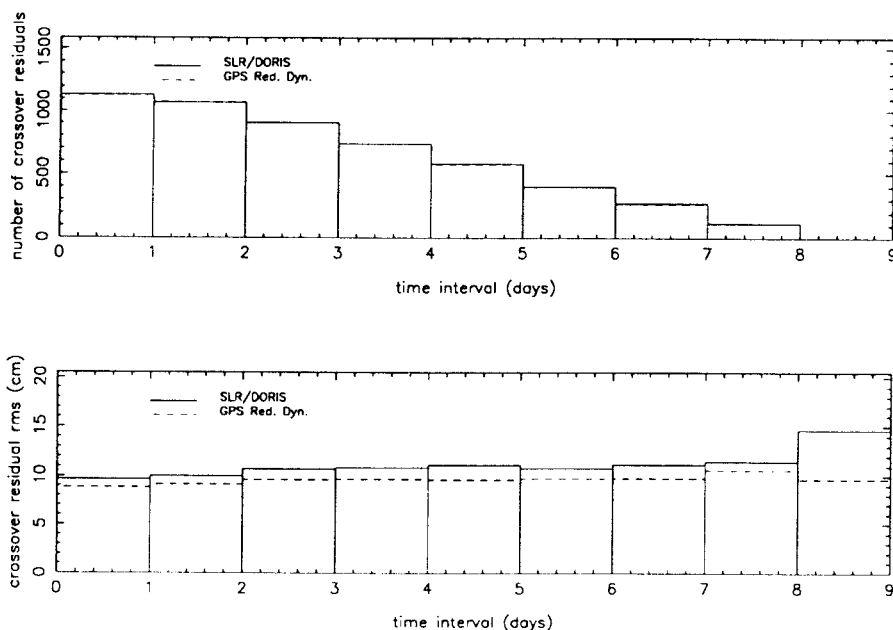


Figure 8. TOPEX/Poseidon crossover residual RMS for cycle 14 vs. time interval between ascending and descending tracks for the SLR/DORIS and GPS reduced-dynamic orbit solutions.

SLR/DORIS orbit solution which is representative for the other dynamic solutions. Because ocean variability and tidal errors get more pronounced on a long-term scale, they cause the crossover residual RMS to steadily increase as the time interval grows larger. The inconsistency towards the end of Figure 8 is due to the fact that the computations in this Section are exclusively based on TOPEX altimeter data. The observations made by Poseidon were considered less useful because this altimeter is only operational for about 10% of the repeat cycle which results in unreliable crossover statistics if altimeter observations of only one cycle are processed. As the last two days of cycle 14 belong to Poseidon, only one TOPEX crossover was found with a time interval of more than 8 days (top of Figure 8).

A possible way to let the crossover residuals enter into the orbit error assessment scheme would be to only select the short-term crossover residuals with a maximum time interval between ascending and descending tracks of e.g. less than 1 day. However, dividing the RMS value of these crossover residuals by $\sqrt{2}$, there still seems to be a significant discrepancy with the predicted 3-5 cm error level. Hence, it must be concluded that even the short-term crossover residuals are seriously affected by ocean variability, tidal errors, and uncertainties in the altimeter corrections. Therefore, a different approach was followed to set up the orbit error budget. A feasible method has been found in dividing the orbit error into two components: (i) gravity-induced orbit error resulting from errors in the gravity field model, and (ii) 1-cpr orbit error which is an ensemble of gravity field errors, epoch state vector errors, and surface force mismodeling errors. The gravity-induced part of the orbit error can be derived from the calibrated covariance matrix of the JGM-2 gravity field model while both the sine and cosine components of the 1-cpr orbit error can be assessed from the crossover residuals.

Orbit errors of gravitational origin Δr can be characterized by an amplitude that is constant in time. As a function of geographic coordinates (λ, ϕ) , these errors can be divided into a mean

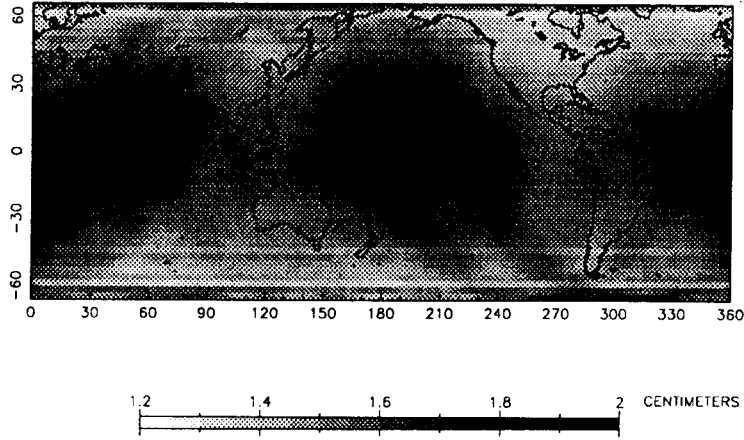


Figure 9. TOPEX/Poseidon geographically-correlated orbit error from JGM-2 covariance, RMS=1.7 cm.

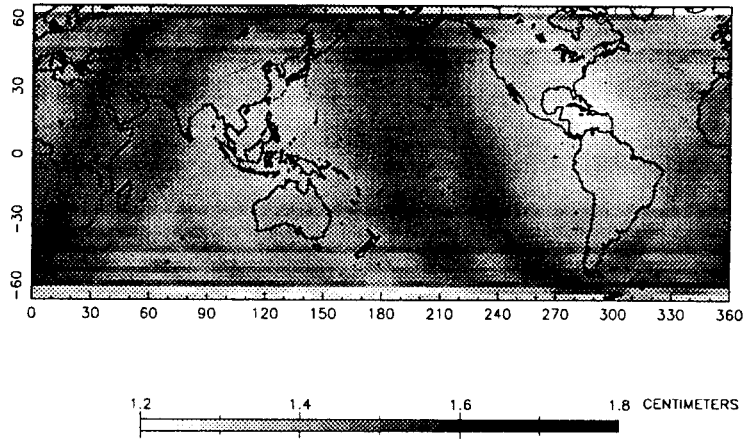


Figure 10. TOPEX/Poseidon variable orbit error from JGM-2 covariance , RMS=1.5 cm.

component Δr_m , and a variable component Δr_v about this mean [7]:

$$\Delta r(\lambda, \phi) = \Delta r_m(\lambda, \phi) \pm \Delta r_v(\lambda, \phi) \quad (1)$$

The positive sign is applied if the satellite moves on an ascending track whereas the negative sign applies to descending tracks. From the above Equation, it can be seen that when computing crossover residuals, where the orbit errors on ascending and descending tracks are subtracted, the mean component will cancel and therefore cannot be observed from the crossover residuals. For this reason, the mean part of the gravity-induced orbit error is also referred to as the *geographically-correlated* orbit error. The variable component on the other hand will appear twice in the crossover residuals:

$$\sigma_{x_o} = 2\sigma_v \quad (2)$$

$$\sigma_r^2 = \sigma_m^2 + \sigma_v^2 \quad (3)$$

where σ_m , σ_v , σ_r , and σ_{x_o} , are the RMS of the mean component, the variable component, the resultant gravity-induced orbit error, and the gravity-induced part of the crossover residuals respectively. To establish the magnitude of the mean and variable components, the Rosborough

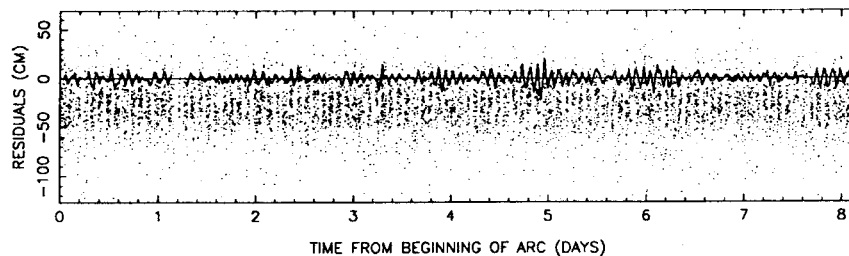


Figure 11. TOPEX altimeter residuals and 1-cpr signal of SLR/DORIS orbit solution for cycle 14. Residuals: mean=-28.9 cm, RMS about mean=24.0 cm, 1-cpr signal: RMS=4.8 cm.

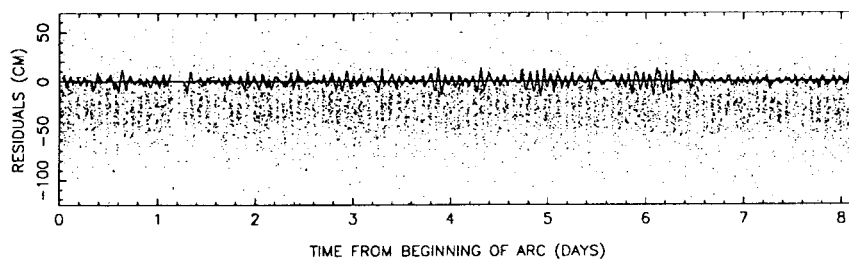


Figure 12. TOPEX altimeter residuals and 1-cpr signal of GPS reduced-dynamic orbit solution for cycle 14. Residuals: mean=-28.2 cm, RMS about mean=23.0 cm, 1-cpr signal: RMS=4.6 cm.

formulation [7] has been applied on a $3^\circ \times 3^\circ$ grid using the JGM-2 covariance (Figures 9 and 10). It was found that the mean and variable parts of the gravity-induced orbit error have an RMS of about 1.7 cm and 1.5 cm respectively. Notice that the mean and variable components are found to be of comparable magnitude which indicates that gravity-induced orbit errors on ascending and descending tracks are uncorrelated and therefore propagate into the crossover residuals by $\sqrt{2}$. Also notice that the gravity-induced orbit error tends to increase over the Pacific and the African continent where satellite tracking data have traditionally been sparse. It should be mentioned that the Rosborough formulation excludes gravity-induced orbit errors due to resonance terms in the gravity field. However, orbit errors produced by these terms are at the 1-cpr frequency and therefore will be absorbed in the orbit determination by the estimated epoch state vector and the 1-cpr acceleration sets.

Orbit error at a frequency of 1 cpr is characterized by day to day amplitude variations of which the cause is twofold. Firstly there are gravitational errors at frequencies of $1 \pm 10/127$ cpr which appear as a daily modulation on the amplitude of the 1-cpr signal. Secondly, 1-cpr acceleration sets are estimated in the orbit determination scheme for each day separately which means that the solved-for accelerations may differ from day to day. Because of these amplitude variations, the 1-cpr orbit error cannot be resolved into a mean and a variable part as was the case for the gravity-induced orbit error. As an alternative, the orbit error at the 1-cpr frequency can be divided into a sine and a cosine component as a function of the argument of latitude. Depicted in Figures 11 and 12 are the altimeter residuals of the SLR/DORIS and the GPS reduced-dynamic orbit solutions for cycle 14 relative to the GRS-80 ellipsoid (semi-major axis: 6378.137 km) and an ocean topography reconstructed from the OSU91A geoid and the DUT-TPXDT94A stationary dynamic topography model [8]. For the reason that the Poseidon altimeter data were excluded from the computations,

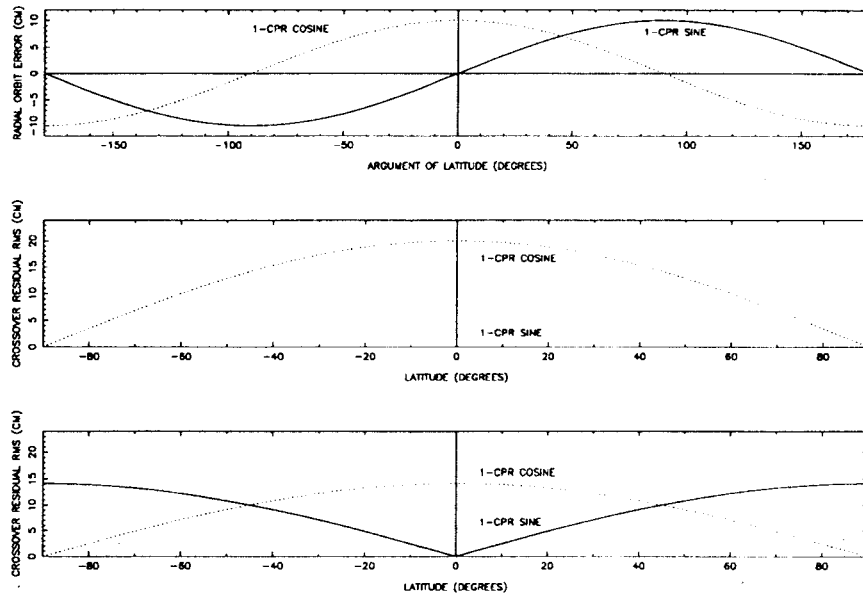


Figure 13. Propagation of 1-cpr orbit error into crossover observations. Top: 1-cpr sine and cosine orbit error with e.g. amplitude=10 cm, RMS=7 cm. Middle: propagation of 1-cpr orbit error with constant amplitude into crossover observations. Sine: RMS=0 cm, cosine: RMS=14 cm. Bottom: propagation of 1-cpr orbit error with varying amplitude (7 cm RMS assumed) into crossover observations. Sine: RMS=10 cm, cosine: RMS=10 cm.

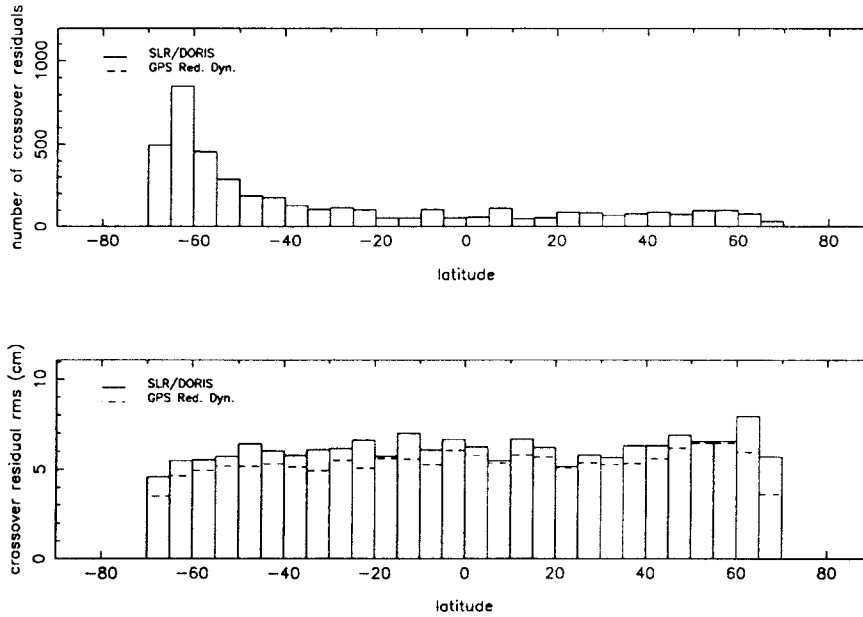


Figure 14. TOPEX 1-cpr crossover residual RMS for cycle 14 vs. latitude of the SLR/DORIS and GPS reduced-dynamic orbit solutions.

only 8 days out of the 10-day repeat cycle are present in Figures 11 and 12. Notice that the value of about -28 cm found for the altimeter bias is related to the adopted reference ellipsoid. Hence, this *relative* altimeter bias should not be confused with the *absolute* altimeter bias of approximately -20 cm that was found by JPL and CNES from the TOPEX altimeter calibration. Also shown as a drawn line in Figures 11 and 12 is the 1-cpr signal that was obtained by performing a frequency demodulation on the altimeter residuals. Clearly visible is the daily modulation on this signal caused by gravitational errors and the estimated sets of 1-cpr accelerations. Notice that because part of the 1-cpr signal in the altimeter residuals can be attributed to errors in the models adopted to represent the ocean topography, it is not possible to directly use this signal for the estimation of the 1-cpr sine and cosine orbit error. Therefore, crossover residuals have to be computed from the 1-cpr signal in the altimeter residuals. From the thus computed 1-cpr crossover residuals, the sine and cosine components can be found.

How the 1-cpr orbit error propagates into the crossover residuals is illustrated in Figure 13. If the 1-cpr sine and cosine orbit error would have had a constant amplitude as shown in the top of this Figure, it would have been possible to distinguish between a mean and a variable part. In that case, it can be easily shown that the sine component would be 100% correlated and therefore becomes the mean that cannot be observed from the crossover residuals, while the cosine component would be 100% anti-correlated (i.e. -100% correlated) and thus becomes the variable part showing up twice in the crossover residuals (middle Figure). For orbit error with a signature as depicted in Figures 11 and 12 however, the amplitude of the sine and cosine components will clearly be different for each orbital revolution. Consequently, the 1-cpr orbit error will decorrelate very rapidly meaning that both the sine and cosine component will show up in the crossover residuals, each component magnified by $\sqrt{2}$ (bottom Figure). As becomes obvious from Figure 13, the average amplitude of the 1-cpr cosine component can be found by dividing the crossover residual RMS at the equator by $\sqrt{2}$. Dividing by another $\sqrt{2}$ will give the RMS of the 1-cpr cosine orbit error. Equivalently, dividing the crossover residual RMS at extreme latitudes by 2 will give the RMS of the 1-cpr sine orbit error. Notice that the middle and bottom curves displayed in Figure 13 apply to a polar orbit. In case of TOPEX/Poseidon, the orbital inclination is 66° so that these curves will not exceed latitudes below -66° and above 66° .

For cycle 14, the 1-cpr signals obtained from the demodulation on the altimeter residuals of the various orbit solutions have actually been used to compute crossover residuals of which the RMS is depicted in Figure 14 as a function of latitude for the SLR/DORIS and GPS reduced-dynamic orbit solutions. Dividing the crossover residual RMS at the equator by 2, the RMS of the 1-cpr cosine orbit error can be estimated at 4.0 cm, 3.0 cm, 3.2 cm, 3.4 cm, and 3.0 cm, for the SLR, DORIS, SLR/DORIS, GPS dynamic, and GPS reduced-dynamic orbit solutions respectively. Dividing the crossover residual RMS at extreme southern latitude by 2, these values for the 1-cpr sine orbit error are respectively 2.7 cm, 1.8 cm, 2.3 cm, 1.7 cm, and 1.7 cm. The extreme southern latitude was chosen as there are significantly more crossover residuals on the southern hemisphere leading to more meaningful statistics (top of Figure 14).

The orbit error components that were discussed in this Section are gathered in Table 5 from which the TOPEX/Poseidon radial orbit error and its contribution to the crossover residuals can be derived. The values of 1.5 cm for the mean and 1.4 cm for the variable part of the gravity-induced orbit error were derived from the JGM-2 covariance matrix but now excluding orbit errors at frequencies of $1 \pm 10/127$ cpr because these have already been accounted for by the 1-cpr orbit error as obtained from the altimeter residuals. Notice that for the gravity-induced error, the same values were assigned to all dynamic orbit solutions. This seems to be a reasonable assumption because the radial differences between these orbit solutions are mainly at the 1-cpr frequency as will be demonstrated in the next Section. In case of the GPS reduced-dynamic solution, it is expected that the larger part of the gravity-induced orbit error has been absorbed by the process-noise force. Also notice that the mean part of the gravity-induced orbit error in Table 5 is not transposed to the crossover column whereas the variable part is transposed twice. Adding all the numbers in the orbit

Table 5. TOPEX/Poseidon orbit error estimate from cycle 14.

Orbit error component	Δ Crossover (cm)					Orbit error (cm)				
	SLR	DORIS	SLR/ DORIS	GPS Dyn.	GPS Red. Dyn.	SLR	DORIS	SLR/ DORIS	GPS Dyn.	GPS Red. Dyn.
Gravity-induced orbit error										
-mean	-	-	-	-	-	1.5	1.5	1.5	1.5	-
-variable	2.8	2.8	2.8	2.8	-	1.4	1.4	1.4	1.4	-
1-cpr orbit error										
-cosine	5.7	4.2	4.5	4.8	4.2	4.0	3.0	3.2	3.4	3.0
-sine	3.8	2.5	3.3	2.4	2.4	2.7	1.8	2.3	1.7	1.7
Total (RSS)	7.4	5.6	6.2	6.1	4.8	5.2	4.1	4.4	4.2	3.4

error column RSS wise, estimates of about 5 cm for the accuracy of the SLR orbit solution, 4 cm for the DORIS, SLR/DORIS, and GPS dynamic orbit solutions, and 3 cm for the GPS reduced-dynamic orbit solution are obtained. These values compare quite well with the 3-5 cm error level as predicted by the radial RMS overlaps and the RMS of fit of the SLR residuals. It can also be seen that the orbit error makes a contribution of only 5-7 cm to the crossover residuals.

5 Orbit comparisons

To investigate the consistency between the various orbit solutions, TOPEX/Poseidon orbits have been created in Precise Orbit Ephemeris (POE) format for cycle 14. Using this cycle, all dynamic orbit solutions have been compared with the GPS reduced-dynamic orbit solution whereas the dynamic solutions have also been compared mutually. Especially the former comparisons are of interest because they give an indication of the orbit error present in the dynamic solutions assuming that the GPS reduced-dynamic orbit is a perfect fit. Figure 15 shows the differences between the TOPEX/Poseidon reduced-dynamic and dynamic orbits from GPS data. As can be seen, these differences have an RMS of about 3 cm radial, 7 cm cross-track, and 9 cm along-track. A comparison between the GPS reduced-dynamic radial ephemeris solution and the corresponding SLR/DORIS dynamic solution is presented in Figure 16. Obviously, the agreement between the radial position components is better than 4 cm in RMS sense. Comparing the TOPEX/Poseidon dynamic radial ephemeris solution from DORIS data with that from SLR data, the RMS difference is about 3 cm, as shown in Figure 17. Since the cross-track and along-track differences for the last two comparisons are of the same order of magnitude as the differences between the TOPEX/Poseidon reduced-dynamic and dynamic orbits from GPS data, it can be concluded that a good orbit agreement is obtained between the various tracking systems and that a good orbit accuracy is achieved for each individual tracking system. Generally, the comparisons of the dynamic orbit solutions against the GPS reduced-dynamic orbit show radial consistencies within 3-4 cm, which compare quite well with the estimated 3-5 cm error level from the previous Sections. From the comparisons between the dynamic orbit solutions, radial consistencies of 2-4 cm have been found. Regarding the fact that the orbits have been computed from different tracking data types, a radial agreement of 2-4 cm may be considered as an extremely good result. From Figures 15 to 17, it is obvious that the main part of the orbit differences can be attributed to a 1-cpr signal resulting from different estimates for the state vector at epoch and differences between the solved-for 1-cpr accelerations.

The radial orbit differences between the SLR/DORIS orbit solution and the GPS reduced-dynamic orbit solution have also been plotted as a function of geographic location on a $5^\circ \times 5^\circ$ grid by averaging all differences in a grid cell (Figure 18). Because there are an equal number of ascending and descending tracks per grid cell and because the geographically-correlated orbit error in the reduced-dynamic orbit solution is expected to be very small, this means that Figure 18 is a measure for the geographically-correlated orbit error present in the SLR/DORIS orbit solution (see Equation 1). Comparing Figures 18 and 9, areas where the radial orbit differences are largest indeed match the areas where the JGM-2 covariance predicts the largest errors. Notice that the discrepancy

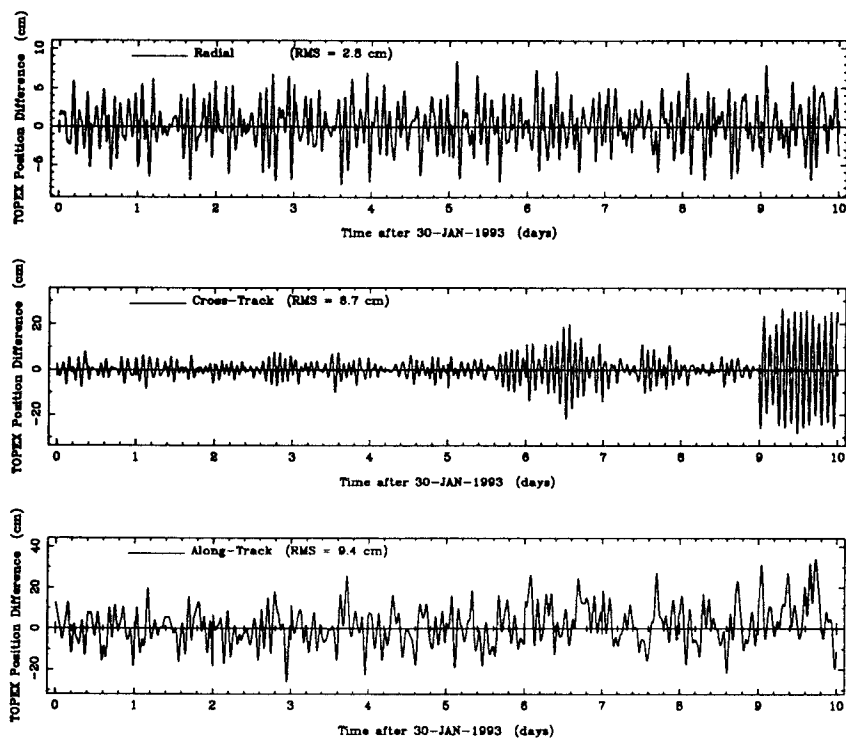


Figure 15. Differences between GPS reduced-dynamic and dynamic orbits for TOPEX/Poseidon cycle 14.

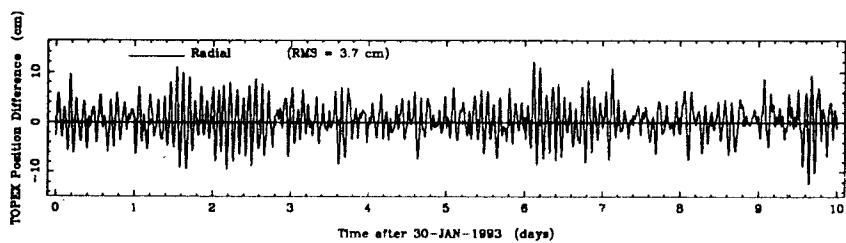


Figure 16. Radial differences between GPS reduced-dynamic and SLR/DORIS orbits for TOPEX/Poseidon cycle 14.

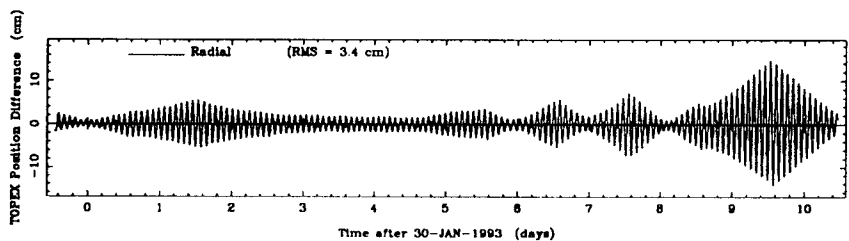


Figure 17. Radial differences between DORIS and SLR orbits for TOPEX/Poseidon cycle 14.

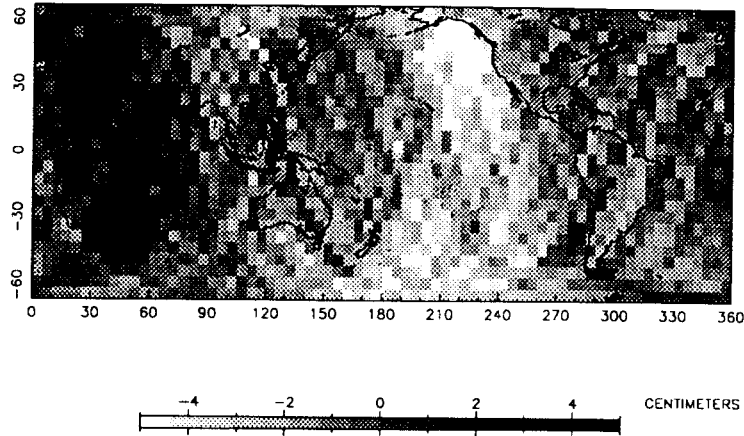


Figure 18. Mean radial differences between GPS reduced-dynamic and SLR/DORIS orbits for TOPEX/Poseidon cycle 14, RMS=2.3 cm.

between the RMS orbit difference of 2.3 cm and the geographically-correlated orbit error predicted by the JGM-2 covariance of 1.7 cm, can be attributed to the 1-cpr signal in the orbits. Due to the rapid amplitude variations however, the 1-cpr signal is somewhat smoothed as a function of geographic location and therefore does not distinctly manifest itself in Figure 18. The outcome of this comparison demonstrates that the JGM-2 covariance matrix has been properly calibrated and gives a reliable estimate of the geographically-correlated orbit error present in the dynamic orbit solutions.

6 Conclusions

Results obtained for the radial RMS overlap and the RMS of fit of the SLR residuals indicate that the TOPEX/Poseidon radial orbit error is within 3-5 cm, which is well below the mission goal of about 10 cm. This estimate is confirmed by an orbit error assessment scheme that implements crossover residuals to estimate the 1-cpr orbit error, and by a comparison between the radial ephemerides of the various orbit solutions. The main part of the orbit differences was found to be of a 1-cpr nature. Furthermore, it was found that for TOPEX/Poseidon, the crossover statistics mainly reflect ocean variability and tidal errors, and that no more than 5-7 cm in the crossover residuals can be attributed to orbit errors. Moreover, about 2 cm of the orbit error is of gravitational origin, while 3-4 cm is caused by errors at the 1-cpr frequency which are a mixture of gravity-induced orbit errors, epoch state vector errors, and surface force mismodeling errors.

References

- [1] K. F. Wakker, B. A. C. Ambrosius, R. C. A. Zandbergen, and G. H. M. van Geldorp, *Precise orbit computation, gravity model adjustment and altimeter data processing for the ERS-1 altimetry mission*, *ESA contract report 6140/84/D/IM*, Faculty of Aerospace Engineering, Delft University of Technology, Delft, The Netherlands, 1987.
- [2] R. C. A. Zandbergen, *Satellite altimeter data processing, from theory to practice*, Ph.D. dissertation, Delft University Press, Delft, The Netherlands, 1990.
- [3] B. H. Putney, J. A. Marshall, R. S. Nerem, F. J. Lerch, D. S. Chinn, C. C. Johnson, S. M. Klosko, S. B. Luthke, K. E. Rachlin, T. A. Williams, R. G. Williamson, and N. P. Zelensky, *Precise orbit*

- determination for the TOPEX/Poseidon mission, *Paper AAS-93-577* presented at the AAS/AIAA Astrodynamics Specialist Conference, Victoria, B.C., Canada, 16–19 August 1993.
- [4] W. Bertiger, S. Wu, T. Yunck, R. Muellerschoen, P. Willis, Y. Bar-Sever, A. Davis, B. Haines, T. Munson, S. Lichten, and R. Sunseri, Early results from the TOPEX/Poseidon GPS precise orbit determination demonstration, in *Spaceflight Mechanics 1993, Volume 82, Part II, Advances in the Astronautical Sciences*, pp. 863–876, American Astronautical Society, 1993.
 - [5] S. C. Wu, R. J. Muellerschoen, W. I. Bertiger, T. P. Yunck, Y. E. Bar-Sever, and T. N. Munson, Automated precision orbit determination for TOPEX/Poseidon with GPS, *AAS paper 93-576* presented at the AAS/AIAA Astrodynamics Specialist Conference, Victoria, Canada, 16–19 August 1993.
 - [6] W. I. Bertiger, Y. E. Bar-Sever, E. J. Christensen, E. S. Davis, J. R. Guinn, B. J. Haines, R. W. Ibanez-Meier, J. R. Lee, S. M. Lichten, W. G. Melbourne, R. J. Muellerschoen, T. N. Munson, Y. Vigue, S. C. Wu, T. P. Yunck, B. E. Schutz, P. A. M. Abusali, H. J. Rim, M. M. Watkins, and P. Willis, GPS precise tracking of TOPEX/Poseidon: results and implications, *J. Geophys. Res.*, 1993, submitted for publication to TOPEX/Poseidon special issue.
 - [7] G. W. Rosborough, Satellite orbit perturbations due to the geopotential, *Report no. CSR-86-1*, Center for Space Research, University of Texas at Austin, 1986.
 - [8] M. C. Naeije, A. J. E. Smith, D. C. Kuijper, R. Scharroo, B. A. C. Ambrosius, and K. F. Wakker, Precise TOPEX orbits in ocean dynamic topography modeling, *J. Geophys. Res.*, 1994, submitted for publication to TOPEX/Poseidon 2nd special issue.